J. Braz. Chem. Soc., Vol. 17, No. 4, 627-642, 2006.
Printed in Brazil - ©2006 Sociedade Brasileira de Química
0103 - 5053 $6.00+0.00

Review

Cathodes for Lithium Ion Batteries: The Benefits of Using Nanostructured Materials

Fernanda F. C. Bazito and Roberto M. Torresi*

Instituto de Química, Universidade de São Paulo, CP 26077, 05513-970 São Paulo-SP, Brazil

As celas de íon lítio disponíveis comercialmente, as quais são as mais avançadas entre as baterias recarregáveis disponíveis até agora, empregam óxidos de metais de transição microcristalinos como catodos, os quais funcionam como matrizes de inserção de lítio. Em busca por uma melhor performance eletroquímica, o uso de nanomateriais no lugar dos materiais convencionais tem emergido como excelente alternativa. Nesta revisão nós apresentaremos uma breve introdução sobre as motivações de usar materiais nanoestruturados como catodos em baterias de íon-lítio. Para ilustrar tais vantagens apresentamos exemplos de pesquisas relacionadas com a preparação e dados eletroquímicos dos mais usados catodos em nanoescala, tais como $LiCoO_2$, $LiMn_2O_4$, $LiMnO_2$, LiV_2O_5 e $LiFePO_4$.

Commercially available lithium ion cells, which are the most advanced among rechargeable batteries available so far, employ microcrystalline transition metal oxides as cathodes, which function as Li insertion hosts. In search for better electrochemical performance the use of nanomaterials in place of these conventional ones has emerged as excellent alternative. In this review we present a brief introduction about the motivations to use nanostructured materials as cathodes in lithium ion batteries. To illustrate such advantages we present some examples of research directed toward preparations and electrochemical data of the most used cathodes in nanoscale, such as $LiCoO_2$, $LiMn_2O_4$, $LiMnO_2$, LiV_2O_5 e $LiFePO_4$.

Keywords: nanotechnology, lithium-ion battery, cathode, nanoparticles

1. Initial Remarks

Since Sony introduced its 18650 cell in 1990,[1] Li-ion batteries with excellent electrochemical performance have been manufactured and occupied a prime position in the market place[2] to power portable and non-portable devices.[3-5] The reason for this relevance is that compared to traditional rechargeable batteries such as, lead acid and Ni-Cd, the lithium-ion battery shows several advantages, such as lighter in weight, smaller in dimension and higher energy density.[1] Moreover, although capacity values may be similar to other rechargeable systems, voltages are approximately three times higher, affording higher energy.[1]

In general, the commercial lithium-ion batteries use graphite-lithium composite, Li_xC_6, as anode, lithium cobalt oxide, $LiCoO_2$, as cathode and a lithium-ion conducting electrolyte. When the cell is charged, lithium is extracted from the cathode and inserted at the anode. On discharge, the lithium ions are released by the anode and taken up again by the cathode (Figure 1).

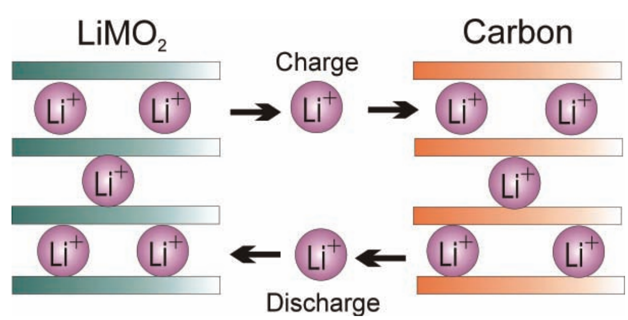

Figure 1. Schematic diagram of a lithium-ion battery.

Owing to the importance of lithium ion batteries, these cells are still object of intense research to enhance their properties and characteristics. The searches focus on all aspects of these batteries, including improved anodes,[6-8] cathodes[9-17] and electrolytes.[18-22] However, most of these efforts are concentrated in new cathode materials, since the most used cathode material ($LiCoO_2$) is expensive and is somewhat toxic.

The active cathode material of a secondary lithium ion battery is a host compound, where lithium ions can be inserted and extracted reversibly during the cycling

* e-mail: rtorresi@iq.usp.br

process. The main requirements for cathode materials are: (*i*) the transition metal ion in the insertion compound cathode should have a large work function to maximize the cell voltage, (*ii*) the insertion compound should allow an insertion/extraction of a large amount of lithium to maximize the cell capacity, (*iii*) the lithium insertion/extraction process should be reversible with no or minimal changes in the host structure over the entire range of lithium insertion/extraction, (*iv*) chemical stability for both redox forms of cathode couple, (*v*) the insertion compound should support good electronic and Li^+ conductivities to minimize cell polarizations and, (*vi*) the voltage profile should be relatively continuous, without large voltage steps that can complicate power managements in devices. Finally, from a commercial point of view, the insertion compound should be inexpensive, environmentally friendly and lightweight to minimize the battery weight.

In the last years, the use of nanomaterials for Li-ion cathodes instead conventional materials has become very attractive to improve the performance of lithium rechargeable batteries. Several groups have shown that nanosized materials are emerging as successful solutions to enhance rate capability and cyclic stability of these electrodes.[23-28] In one paper published in 2003, Bueno and Leite[29] discuss the effects of the nanocrystalline state on the performance of Li-ion batteries in a conceptual point of view, where two types of size effects are discussed: (*i*) trivial size effects which rely on solely on the increased surface to volume ratio and (*ii*) true size effects, which also involve changes of local materials properties. Based on this paper and other reviews, motivations for using nanomaterials will be discussed.

Nanoparticles have critical nucleation radii (CNRs) that are larger than the particle diameter. Since the structural transitions to thermodynamically undesired structures can only occur if the particle radius is larger than the critical nucleation radius for that phase,[30] it is possible to eliminate such transitions by using nanoparticles with CNRs larger than the particle radius. Thus, small particles would accommodate more easily the structural changes occurring during the cycling process where lithium are inserted and extracted.

In nanoscopic particles the charge accommodation occurs largely at or very near the surface and the smaller the particles are, the larger the portion of these constituent atoms is at the surface. For example, for a 1 nm MnO_2 particle, the fraction of Mn(IV) ions at the surface will be 0.5, while for a 10 nm particle it will be 0.05. Further, for a 10 nm particle the fraction of Mn(IV) ions within next-nearest neighbor distance of the surface is 0.75. This fact will reduce the need for diffusion of Li^+ in the solid phase, greatly increasing the charge and discharge rate of the cathode. This will also reduce the volumetric changes and lattice stresses caused by repeated Li^+ insertion and expulsion.[31,32]

The Li^+ diffusion distances will be significantly reduced and Li^+ diffusion within the particle to compensate reduction of non-surface cation sites. For example, for a 10 nm particle and a bulk diffusion coefficient of Li^+ in typical insertion materials of approximately 10^{-10} cm^2 s^{-1},[33] the time required for Li^+ to diffuse a distance equal to the particle radius is 2.5×10^{-3} s. Thus, Li^+ diffusion within the particle to compensate reduction of non-surface Mn sites is not a significant kinetic barrier during cycling. At high discharge rate, high Li^+ ion insertion flux density and slow Li^+ transport result in concentration polarization of lithium ion within the electrode material. This causes a drop in cell voltage, which results in termination of the discharge before the maximum capacity of the electrode materials is used. Decreasing the average diffusion distance, while keeping the mass constant, increases the surface are of the electrode and lowers current density. This results in the delay of concentration polarization to higher current values and, consequently, increased electrode rate capability.

Numerous materials have been studied for use as lithium ion battery cathodes, including metal oxides, metal sulfides, conducting polymers and poly(sulfides). Among them, transition metal oxides are the most successful materials because of their chemical and structural stability, high lithium ion capacity and favorable electrical properties, such as high conductivity of lithium ions and electrons.

Since Mizushima *et al.*,[34] in 1980, have proposed the use of layered $LiCoO_2$ as an intercalation cathode, the use of layered transition metal oxides, including two-dimensional layered oxides $LiCoO_2$, $LiNiO_2$, $LiMnO_2$ and LiV_2O_5 and the three dimensional spinel $LiMn_2O_4$ has become well established and several groups have focused their researches on the maximization of the electro-chemical properties of these existing materials.[35-39] In addition, recently the olivine $LiFePO_4$ was proposed as possible cathode as lithium ion batteries.[40]

In layered $LiMO_2$ (M=Co, Mn), the lithium and the metallic (M^{3+}) ions occupy alternate (111) planes of the cubic rock salt structure. The lithium ion intercalates into or deintercalates reversibly from the MO_2 layers. Spinel $LiMn_2O_4$ has a cubic spinel structure ($Fd\bar{3}m$), where Li^+ ions occupie the **8a** tetrahedral sites with manganese occupying the octahedral **(16d)** site and the other octahedral site **(16c)** is vacant. When Li^+ diffuses within the structure, first it moves from the **8a** site to the neighbor empty octahedral **16c** site, then to the next **8a** site in such a way that the Li^+ ion takes the diffusion path **(8a-16c-8a)**. The olivine structure of $LiFePO_4$ has a hexagonally-close-packed oxygen array with corner-shared FeO_6 octahedral and PO_4 tetrahedral. The lithium ions are octahedrally coordinated to oxygen, forming edge-sharing chains of LiO_6 octahedral (Figure 2).[41] In a lithium cell, electrochemical extraction of lithium from $LiFePO_4$ is accompanied by a direct transition to $FePO_4$, in which the Fe^{2+} ions are oxidized to Fe^{3+}, leaving the olivine $FePO_4$ framework intact. The diffusion pathway for the lithium ions in $LiFePO_4$ was only recently discussed in one paper where one dimensional diffusion mechanism is proposed, distinctly from the two-dimension diffusion plane observed in layered transition metals oxides and the three-dimensional diffusion channels in spinel $LiMn_2O_4$.[42]

In general, bulk transition metal oxides are prepared by solid-state reactions, which involve repeated heat process at high temperatures. Such processes generally afford the thermodynamically more stable phases and in general, microcrystalline materials are obtained. Because of these undesirable aspects, several methodologies, such as co-precipitation, sol-gel process with/without template, synthesis by precursor, ion-exchange reaction and hydrothermal, which use lower temperature processing and mild conditions have been tested in order to obtain particles with better control of morphology and smaller size.

This review will focus on the preparation and electrochemical performance of nanostructured transition metal oxides commonly used in lithium ions batteries.

2. Lithium Iron Phosphate

Lithium iron phosphate, $LiFePO_4$, is one of the most recent materials reported as cathode for lithium ion battery.[40] Perhaps, a reason that has contributed to this delay is that $LiFePO_4$ has structure significantly different from layered and spinel lithium metal oxides. Fe-based cathode materials are environmentally compatible, cheap, simple in processing and thermal stability comparable to those of $LiCoO_2$, $LiNiO_2$ and $LiMn_2O_4$.[43,44]

$LiFePO_4$ can act as cathode material due to its high discharge potential around 3.4 V versus Li/Li^+ and moderate theoretical capacity (170 mA h g^{-1}).[40] In spite of these advantages, the olivine $LiFePO_4$ presents low conductivity (σ~10^{-9} S cm^{-1}) and thereby its electrochemical performance is limited, resulting in poor rate capability.

In order to enhance and optimize the electronic conductivity of $LiFePO_4$, several groups are dedicating their researches to these materials. Up to now, there is no way to change intrinsically the electrical conductivity of $LiFePO_4$. Thus two alternative methods have been reported. One is the reduction of the grain size of the sample and consequently the diminution of the diffusion length, both for electrons and ions[45] and the other is the manufacture of nanocomposites of $LiFePO_4$ with a conductive phase, such as carbon.[46]

Usually, bulk $LiFePO_4$ is prepared by solid-state methods, where a stoichiometric mixture of iron compound, ammonium dihydrogen phosphate, $NH_4.H_2PO_4$, and lithium hydroxide is heated and calcined several times.[47] Depending on the synthetic conditions, the capacity of the $LiFePO_4$ can reach high values, such as 115 mA h g^{-1}.[48]

Recently, nanocrystalline $LiFePO_4$ powders were prepared by two different methods. One has involved the heating of amorphous nano-sized $LiFePO_4$, prepared by chemical lithiation of amorphous $FePO_4$, at 550 °C, for different periods[49] and the other was a liquid phase methodology.[50] The nanoparticles (100-150 nm) prepared by the first method have shown excellent capacity of 160 mA h g^{-1} with marked capacity loss. The same material prepared by the second methodology (5-50 nm) has exhibited structural stability with no capacity loss during

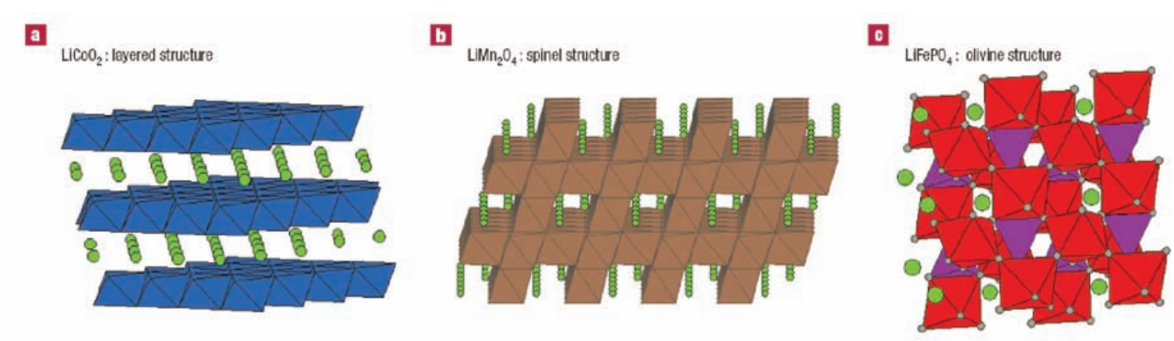

Figure 2. Layered, spinel and olivine structures of positive electrode materials for lithium batteries. Reprinted by permission from Macmillan Publishers Ltd., copyright (2002).[41]

cycling process, in spite of its low specific capacity (90 mA h g^{-1}).

In the search for better performance (higher capacities and cyclability), the preparation of composites of $LiFePO_4$ and carbon in nanoscopic scale to improve their electronic conductivity has emerged as excellent alternative.

These nano-sized $LiFePO_4$/C composites were prepared by different methods, such as, modified solid state reaction,[46] liquid-based method using sugar as carbon source,[51] emulsion drying process[52] and citric acid based sol-gel route.[53] In general, these nanocomposites have shown excellent performance, both in terms of specific capacity and capacity retention. Large agglomerates with hard definition of these nanoparticles $LiFePO_4$ and carbon were observed (Figure 3). The samples synthesized by solid-state reaction have shown larger particle size and poor particle size distribution due to the successive calcinations.

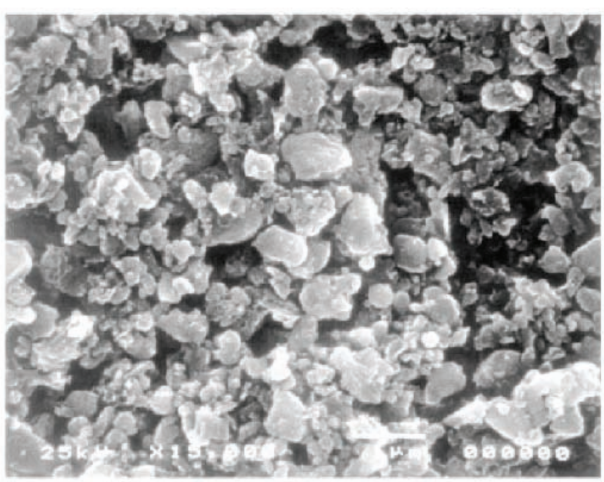

Figure 3. SEM photograph of $LiPO_4$/C composite prepared by liquid-based method. Reprinted with permission from © 2004, Elsevier.[51]

Both the small particle size and the enhanced electronic conductivity were responsible to the higher capacity retention upon cycling and the superior rate capability. Moreover, the carbon addition should not affect the structure of the nanocomposite but probably improves its kinetics in terms of capacity and cycling life due to the intra and inter conductivity of the particles. The addition of carbon can also act as nucleation sites for the growth of $LiFePO_4$ particles, resulting smaller particles.[51,52,54]

3. Vanadium Oxides

Vanadium forms several binary oxides. Among several known vanadium oxides, metastable oxides designated as VO_2(B), V_6O_{13}, V_2O_5 and V_3O_8 are the most interesting cathodes for lithium ion batteries.[55-58]

Among these vanadium derivatives, the layered vanadium pentoxide, LiV_2O_5 has been the most studied in spite of its low discharge voltage, low electric conductivity and slow diffusion kinetics of lithium ion.[59, 60]

To improve the performance of cells employing vanadium pentoxide as cathode several tricks have been tested, including the use of aerogels,[61-63] xerogels,[64-66] nanocomposites of LiV_2O_5 with electronically conducting organic polymers[17,60,67-78] and nanostructured materials (nanotubes, nanorods and nanoparticles).[79-81]

In general, nanotubes of V_2O_5 are prepared by sol-gel method from the hydrolysis of vanadium (V) triiso-propoxide.[82-84] Some authors have used hexadecylamine[82,83] as templating molecule while others microporous polycarbonate filtration membranes.[84] The electrochemical data obtained of the material prepared in presence of the primary amine have shown marked fading under cycling, probably due to the presence of residual organic material. This problem is avoided when synthetic membranes are used as template and initial capacity higher than 200 mA h g^{-1} and excellent reversibility for at least 100 cycles were showed. XRD data have indicated that the tubular structure is preserved, even after prolonged cycling.

In addition to the well-known synthesis of vanadium pentoxide nanotubes starting from vanadium (V) alkoxides, two alternative routes by using two novel non-alkoxide reagents, such as $VOCl_3$ and commercial V_2O_5 as vanadium source and primary amines as templates or intercalates were proposed.[85] The advantages of these methods are low cost and easy handling of commercial V_2O_5. The morphology and the composition of these nanotubes are quite similar to those obtained by vanadium (V) alkoxides. The average lengths were smaller than other nanotubes synthesized using conventional starting material.

V_2O_5 nanoparticles synthesized by combustion flame–chemical vapor condensation process have presented 30% higher retention capacity than conventional materials and up to 50% in case of lower discharge voltage. Initial specific capacities of the nanocrystalline and commercial V_2O_5 material of 390 mA h g^{-1} and 350 mA h g^{-1} have reached 310 mA h g^{-1} and 190 mA h g^{-1}, respectively after eight cycles, showing that the capacity loss is much lower for nano-V_2O_5 than for commercial V_2O_5.[50]

In order to enhance the intrinsic electric conductivity of vanadium pentoxide, nanocomposites of V_2O_5 and conducting polymers or carbon have been target of study, mainly those prepared as nanostructured materials.

There are two different nanocomposites of vanadium pentoxide described in the literature. One is composed of nanofibers of vanadium pentoxide and a conducting polymer, polyaniline[78] while the other uses single-wall carbon nanotubes (SWNTs) to electrically "wire" the poorly conducting V_2O_5 nanoparticles.[86] It is notable that the V_2O_5/SWNT composite has shown much better performance than that obtained with poly(aniline), both in terms of specific capacity as in capacity retention. From the TEM images (Figure 4), it is possible to note that the V_2O_5/SWNT nanocomposite possesses high pore volume that ensures electrolyte access throughout the electrode, while in the V_2O_5/PANI composite a more compact structure is observed. In addition, we believe that the appreciable mechanical property of the SWNT and the electric conductivity between the vanadium pentoxide nanofibers are much more effective than the connectivity promoted by polyaniline. Probably, the addition of carbon nanotubes provides electronic conduction without blocking electrolyte access to the V_2O_5 nanofibers.

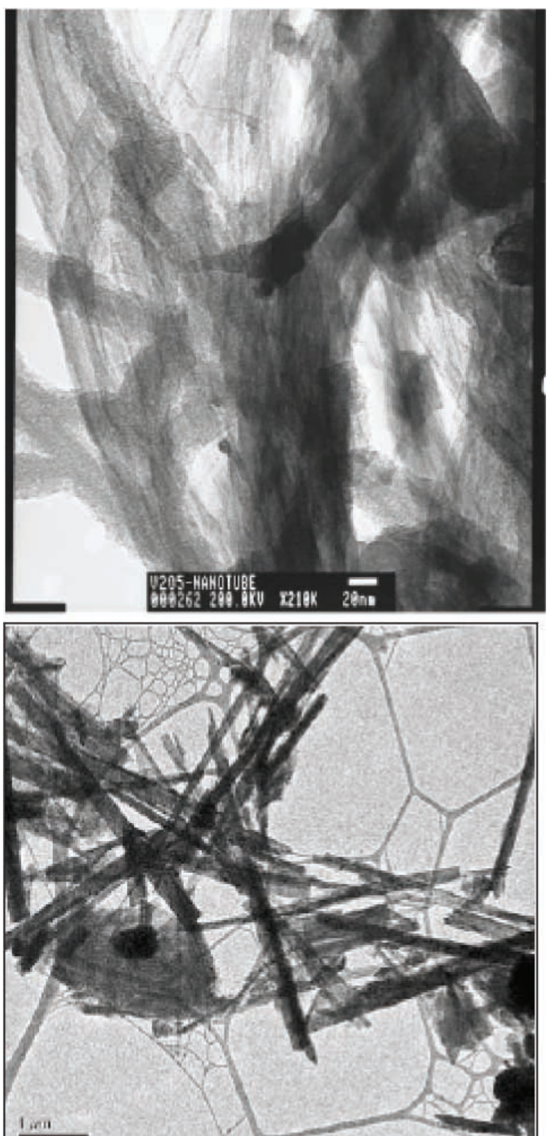

Figure 4. TEM images of V_2O_5/SWNT nanocomposites (left) (Reproduced with permission from © 2002, The Electrochemical Society, Inc. [86]) and V_2O_5/PANI nanocomposites (right) (Reprinted with permission from © 2003, Elsevier[78]).

This argument is corroborated by the comparison between nanocomposites of V_2O_5 with carbon black and single-wall carbon nanotubes. It believes that the traditional composite with carbon black particles forms aggregates, which may occlude the vanadium oxide surface (Figure 5), like the nanocomposites prepared with the conducting polymer, PANI. In the case of V_2O_5/SWNT nanocomposites in spite of the intimate contact between the two components, the access to the electrolyte is facilitated, improving the electrochemical performance of the resulting cell. This structural difference of nanocomposites with SWNT and other compounds is due to the similar morphology and dimensional scale of the SWNT and the prepared vanadium oxide.[87]

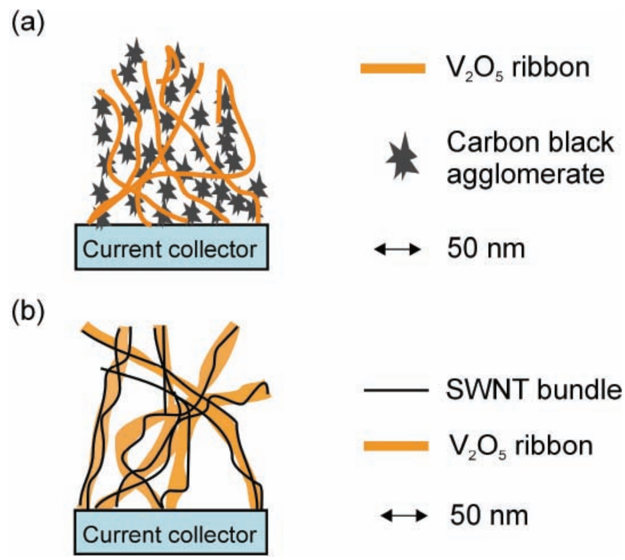

Figure 5. Morphologies for vanadium oxide with carbon black (a) with single-wall carbon nanotubes(b). Reprinted with permission from © 2003, Elsevier.[87]

Another vanadium oxide containing V^{5+} ions that has received much attention is LiV_3O_8. This compound is formed by distorted $[VO_6]$ octahedral sites connected via shared edges and vertices to form $[V_3O_8]^-$ strands that are stacked one upon another to form quasi-layers, where lithium ions are situated. During lithiation V_3O_8 framework remains intact and there is no change in the unit cell volume. These features are attractive to possible use as cathode in lithium ion batteries.[88,89]

The conventional method used to prepare LiV_3O_8 involves the reaction between Li_2CO_3 and V_2O_5 at high temperature.[58,90-93] In general, large particles are obtained due to the use of high temperature.

It is well known that the synthetic procedures as well as the post treatments have significant influences on the electrochemical properties of LiV_3O_8. Several reports have mentioned the importance of both crystallinity and particle size on the electrochemical properties of this material.[94]

LiV_3O_8 nanorods were prepared by a mixture of LiOH, V_2O_5 and NH_4OH after hydrothermal reaction, followed by evaporation and posterior calcinations at different temperatures.[95] The sample heated at 300 °C has afforded the best electrochemical performance, showing high discharge capacity of 300 mA h g^{-1} in the range of 1.8 – 4.0 V and 92% of capacity retention after 30 cycles (Figure 6). Notably, the value of 300 mA h g^{-1} is considerably higher than the capacities of 220-270 mA h g^{-1} obtained for LiV_3O_8 prepared by other methods.[58,90,96,97] TEM micrographies and XRD data have showed that heat treatment performed at high temperatures cause changes in the LiV_3O_8 crystallinity and morphology and larger and more crystalline particles are obtained at 600 °C. Both the small size and the disordered structure are responsible for this appreciable electrochemical response.

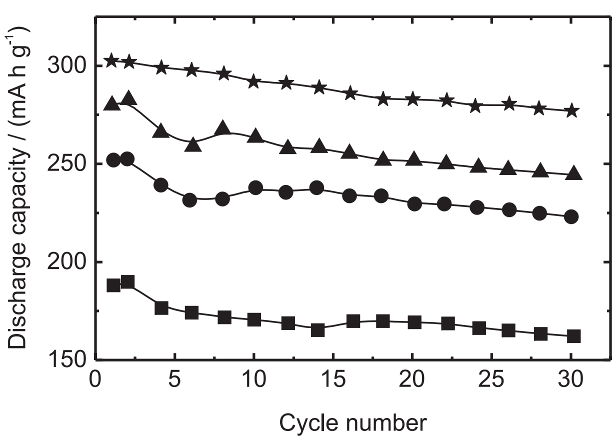

Figure 6. The cycle performance of the cells with LiV_3O_8 heat-treated at (★) 300 °C; (▲) 350 °C (●) 400 °C and (■) 600 °C. Current density: 0.3 mA cm^{-2} Voltage window: 1.8-4.0 V. Reprinted with permission from © 2004, Elsevier.[95]

VO_2(B) has been emerged as another good option as cathode material for lithium ion batteries since 1996.[98] Its structure is built up by distorted octahedral VO_6 that shares both corners and edges, where lithium ions can occupy both octahedral and tetrahedral sites. Commonly, VO_2(B) is obtained from the reduction of potassium vanadate (K_3VO_4) using potassium borohydride in aqueous media. When this compound is heated above 350 °C, it begins to transform irreversibly to the more stable rutile VO_2 (R) as revealed by XRD data, which is not an attractive cathode.[99] Because of this, the methodology to synthesize VO_2(B) is the key point and the search for new methods is still object of interest.

Following this conventional methodology, VO_2(B) metastable was prepared using two different reducting agents, such as KBH_4 and sodium dithionite.[56,100] The observed capacities were higher than that of bulk VO_2(B).[101] In addition, comparing the electrochemical performance of lithium cells using these two samples of VO_2(B), it is evident that the powder prepared with sodium dithionite in LiOH medium has exhibited slight higher capacity than the sample prepared with KBH_4.

Using a surfactant-assisted hydrothermal method at 180 °C, vanadium dioxide nanorods were also prepared.[102] When they are used as cathode, the resulting cell has shown initial discharge specific capacity of 306 mA h g^{-1} at 3.6-1.5 V, which value is significantly superior to those obtained with nanoparticles prepared by Kannan *et al.*[56,100] This nanorod can maintain 80% of its initial capacity.

4. Lithium Cobalt Oxide

The most used transition metal oxide as cathode in commercial lithium-ion cells is layered $LiCoO_2$. Lithium cobalt oxide was suggested for the first time as cathode in 1980[34] and ever since it has been widely investigated due to its favorable electrochemical properties, such as structural stability under cycling and its easy preparation with high quality. However, this material is very expensive and its theoretical capacity is relatively low (~ 130 mA h g^{-1}), since the cobalt system goes through several phases as the lithium content varies from 1 to 0 and in practice it cycles just 0.5/Co.[103]

In general, $LiCoO_2$ is prepared by solid state reaction at high temperature. This methodology is a simple and an inexpensive method, the precursor being simply ground and mixed together before being calcined at high temperature. Solid state reactions to afford $LiCoO_2$ may start from many different precursors, such as, Li_2O and CoO, Li_2CO_3 and Co_3O_4, Li_2CO_3 and Co, LiOH and Co_3O_4 and others, but independent of Co precursor, $LiCoO_2$ formation reaction goes through the reaction of Li precursor and Co_3O_4.[35] Owing to insufficient mixing, low reactivity of the starting materials and calcinations at 850-900 °C for several hours, $LiCoO_2$ produced by solid state reactions usually has non-homogeneity, irregular morphology and a broad particle size distribution, which characteristics influence significantly on the electrochemical properties of the product. Taking into account these advantages, alternative methodologies for the solid-state preparations are been proposed in order to synthesize lithium cobalt oxides at micrometer scale, such as sol-gel,[104-109] water-in-oil emulsion process,[110] emulsion drying method,[111] and electrostatic spray deposition.[112-114] Although these methods require a much lower calcination time and shorter calcination temperature, the synthesis of particles with size under 100 nm is very hard due to their tendency to agglomerate; therefore, the search for new synthetic methodologies or even the modification of the old ones is still necessary.

Recently, the use of triblock copolymer surfactant poly(ethylene oxide)-block-poly(propylene oxide)-block-poly(ethylene oxide) (P123) as soft template agent to synthesize nanosized $LiCoO_2$ by modified sol-gel method was proposed.[115] The size of the sample was around 50-100 nm, depending on the calcinations temperature (Figure 7). Samples prepared at 850 °C have presented the highest initial discharge capacity (150 mA h g^{-1}) with good cycling stability (Figure 8). In spite of the larger size, the samples calcinated at higher temperatures have showed higher charge/discharge capacities, due to their better crystalline structure, which is verified by XRD data.

Another method used to prepare $LiCoO_2$ nanoparticles was the co-precipitation in ethanol with mechanical stirring and posterior calcinations at different temperatures.[116] This method has produced nanoparticles with shape of thin polygons and size in the range of 20-100 nm, the particle size increasing with the temperature. The electrochemical performance of a cell based on these nanoparticles was excellent even at high discharge rate. To illustrate, specific capacities around 100 mA h g^{-1} for a 50 C and 130 mA h g^{-1} for 10 C rates were obtained. The capacity retention was moderate, showing 75% of retention in the 16^{th} cycle. The problem herein is that the nanometer sized lithium cobalt oxide is very easy to agglomerate and thereby it is hard to disperse and mix it with carbon black and binder to produce the cathode. Thus, the contact resistance of a cathode using this nano-size $LiCoO_2$ is much higher than that of commercial one, which explains the pronounced capacity fading.

Besides the low capacity discharge, $LiCoO_2$ goes to thermal decomposition. This instability is due to the reactive tetravalent Co in the delithiated state. Above 150 °C, such material collapses, which reaction is exothermic and the energy stored in the battery is released as heat. During collapse, oxygen is released, which can combust the organic electrolyte and evolve more heat.[117,118] In order to overcome this obstacle, the modification of $LiCoO_2$ by coating a metal oxide on the surface of $LiCoO_2$ particles is a suitable option.[119-123]

In the search for new coatings, aluminum phosphates ($AlPO_4$) have been pointed out as a good alternative coating due to more uniform coating layer when compared to other coatings (Al_2O_3 and ZrO_2). Moreover, the thermal stability of the $AlPO_4$ coated $LiCoO_2$ was comparable to that of $LiMn_2O_4$, which is the most stable compound thermally. The reason to explain why $AlPO_4$ nanoparticle-coated $LiCoO_2$ has superior performance to bare $LiCoO_2$ or other metal-oxide coated cathodes, may be attributed to the strong P=O bond, which is very resistant to chemical attack. The direct coating of $AlPO_4$ nanoparticles on

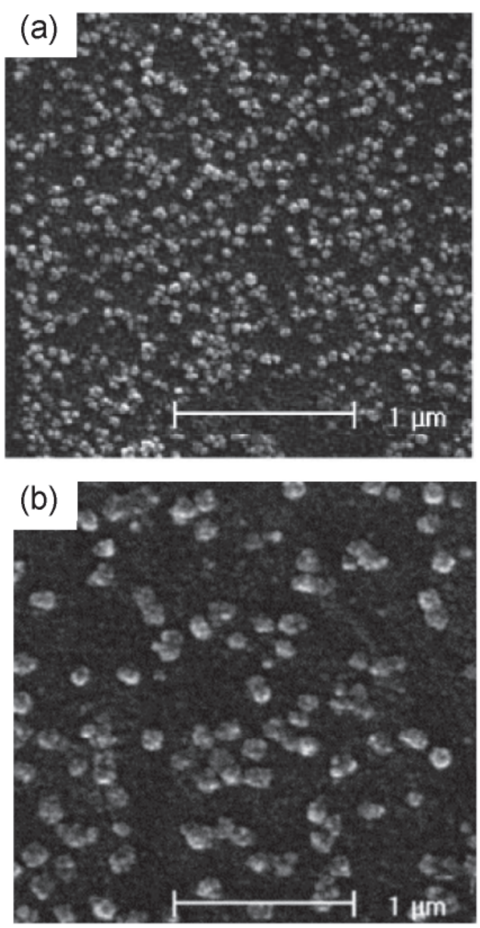

Figure 7. SEM images of $LiCoO_2$ calcined at various temperatures (a) 450 °C and (b) 850 °C for 12 h. Reprinted with permission from © 2005, Elsevier.[115]

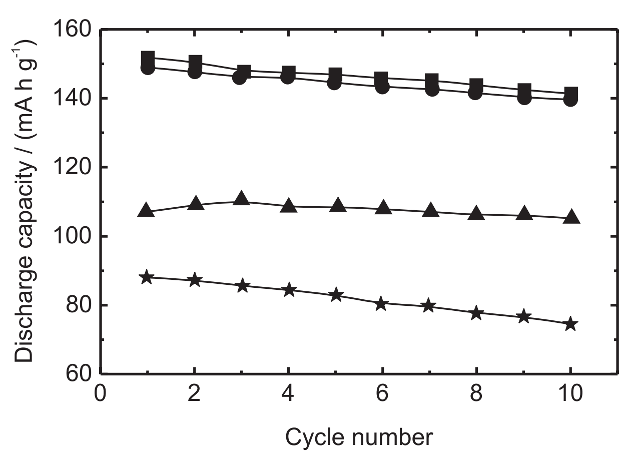

Figure 8. Discharge capacity at different cycle number for $LiCoO_2$ samples calcined at various temperatures: (★) 450 °C (▲) 600 °C (●) 750 °C and (■) 850 °C for 12 h. Reprinted with permission from © 2005, Elsevier.[115]

$LiCoO_2$ nanoparticles has shown a drastic improvement in both the safety and the electrochemical properties of $LiCoO_2$ cathodes.[124] Up to now, the $AlPO_4$-nanoparticle coated $LiCoO_2$ has shown approximately 99% retention of capacity (150 mA h g^{-1}) at 1 C, even after 20 cycles. The increase in the thickness of the $AlPO_4$ coating has led to improvements of the electrochemical performance and the thermal stability.[125,126] Figure 9 shows the retention capacity and some Co dissolution from bare and coated cathodes after 50 cycles. Cobalt dissolution from coated cathodes was significantly reduced when compared with the bare sample. Based on these results, the retention capacity appears to correlate with the Co dissolution suppressed by the $AlPO_4$ nanoparticles.

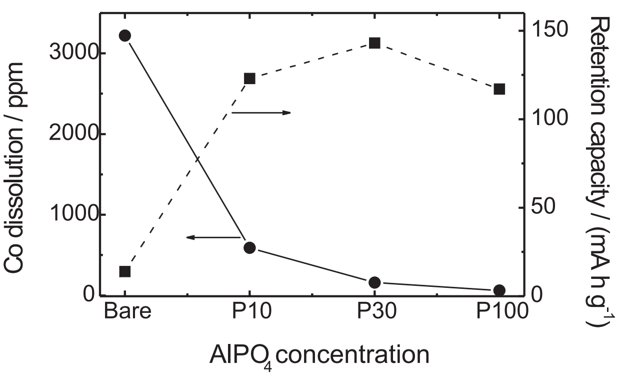

Figure 9. Plot of the retention capacity and Co dissolution in the bare and $AlPO_4^-$ coated $LiCoO_2$ cathodes. Reprinted with permission from © 2003, Elsevier.[125]

Besides the aluminum phosphates coatings, MgO nanoparticles were also tested as protective layer in $LiCoO_2$. Zhao *et al.*[127] have reported the deposition of nanocrystalline MgO on commercial $LiCoO_2$ *via* sol-gel method. During heat treatment and charge-discharge process, Mg^{2+} ions have diffused into the $LiCoO_2$ layers, acting as a pillar between CoO_2 layers and stabilizing the initial structure. The electrochemical performance of this modified $LiCoO_2$ has shown initial discharge capacity of more than 130 mA h g^{-1} maintained even after 40 cycles, while only 13 mA h g^{-1} for pristine $LiCoO_2$ was registered (Figure 10). These electrochemical results are a quite similar to those obtained for $AlPO_4$ coated $LiCoO_2$ electrodes; however the thermal stabilities of the latter samples were much more pronounced. The addition of a large amount of MgO (above 1% mol) is not favorable, since this compound is not electroactive.

5. Manganese Oxides

The use of manganese oxides in rechargeable lithium cells has been stimulated due to their low cost and small environmental impact. In this review, we will be centered on the spinel phase ($LiMn_2O_4$) and on layered manganese oxide ($LiMnO_2$).

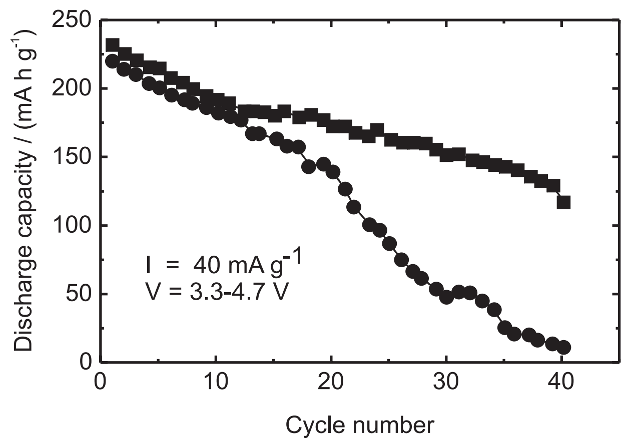

Figure 10. Cycling stability curves of pristine $LiCoO_2$ (●) and 1 mol% MgO-coated $LiCoO_2$ (■). Potential range: 3.3-4.7 V. Reprinted with permission from © 2004, Elsevier.[127]

The discharge curve for $Li_xMn_2O_4$ has two concentration portion (Figure 11), occurring near 4 V (region I and II) and 3 V (region III), which correspond to the addition of one more lithium, resulting in $Li_2Mn_2O_4$.[128,129] In the composition range, $0<x<1$, at 4 V, the structure of $Li_xMn_2O_4$ remains cubic. At 3 V, in the composition range $1.0<x<2.0$ the cubic spinel phase transforms into an ordered tetragonal rock-salt phase, NaCl-type structure.

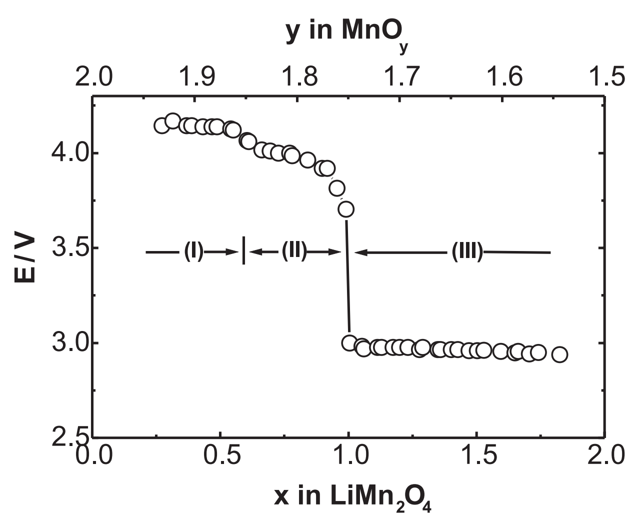

Figure 11. Open circuit curve of $Li_xMn_2O_4$ at 30 °C. Reprinted with permission from © 2001, Elsevier.[128]

The spinel phase only cycles well for 0.5 Li/Mn, since discharge process for this material is normally limited to the upper plateau around 4V. The principal reason for the degradation at potentials below 3.5 V is presumably the transition from cubic phase to tetragonal phase. One more reason attributed to the poor cycle life of $Li_xMn_2O_4$ in the 3V plateau is the asymmetry of expansion and compression processes observed in the $Li_xMn_2O_4$ lattice during cycling, due to the Jahn-Teller effect.[130-133]

Traditionally, spinels are produced by annealing lithium compounds (LiOH, Li_2CO_3, Li_2NO_3, LiI) with manganese oxides, acetates or hydroxides. This annealing process, done in air at high temperature, affects both morphology and structural characteristics of the target product. These conventional solid state methods are not relevant to produce nanosized spinel $LiMn_2O_4$, since repeated heat treatments at high temperatures are necessary, which leads to large particle size, inhomogeneity, irregular morphology and broad particle size distribution.[134-137] Thus, a sustained effort of many researchers has gone into the development of new synthetic methods to yield nanocrystalline $LiMn_2O_4$ particles, such as acetate based chemical solution route,[138] reduction of manganese dioxide by glucose,[139] modified citrate route,[140] ultrasonic spray pyrolysis,[141] sol-gel using citric acid,[142] nitrate based chemical solution route,[143] mechanochemical synthesis,[144] sol-gel method,[27] self-combustion reaction,[145] glycine nitrate combustion process[146] and solid state reaction followed by ball milling.[147]

Depending on the synthetic procedure, nanosized $LiMn_2O_4$ with different physical and chemical properties, such as crystallinity, amount of combined water, specific surface area, porosity and conductivity were obtained. These characteristics affect the electrochemical properties of a resulting cell using these materials as cathodes, but it is certain that their small size is crucial to improve the electrochemical performance compared with batteries using conventional microcrystalline particles.

In general, the procedures listed above have produced nanoparticles with grain size ranging from 10 to 150 nm. In some cases, it is clearly seen that large particles consisted by several agglomerate nanocrystallines were obtained.[138,147] Even in these cases, in spite of the large size, due to the presence of nano-size sub-grains inside the relatively large particle, the performance electrochemical is better than the results obtained for bulk $LiMn_2O_4$. After calcinations at different temperatures, it was observed that at high temperatures, larger particles and more crystallinity were obtained (Figure 12). To illustrate, the XRD patterns of the spinel $LiMn_2O_4$ prepared by self-combustion reaction (SCR) calcinated at different temperature are shown in Figure 13.[145] Further heating at higher temperature leads to gradual sharping of the diffraction peaks, which is an indicative of improved crystallinity of the samples. This fact was also confirmed by detailed analysis of the peak broading combined with SEM.[145] The discharge capacity values have varied from 100 to 150 mA h g^{-1} at 4 V in most of the cells using these nano-sized $LiMn_2O_4$. However, the capacity retentions have varied accentually depending on the sample used. For example, the batteries using nanoparticles produced by acetate based chemical solution route[138] have shown severe capacities fading. For the other cases, the capacity retention was much high, ranging from 70 to 90% after several cycles. Such difference among nano-sized samples might be related to the uniformity of particles shape and size. In other words, a cathode consisting of homogeneous particle is expected to have a regular network which can maintain a uniform intercalation reversibility of each particle through repeated cycles. On the contrary, heterogeneous and partially agglomerated particles may have different reactivity, which disparity among particles with various sizes is considered to increase as the cycling proceeds, resulting in a decrease in the reversibility of the electrode. The nanoparticles produced by solid state reaction followed by ball milling process have demonstrated almost no capacity fading, showing that this process significantly changes particle characteristics not only on the formation of nanometer-scale grains in an agglomerate particle, but also on the generation of lattice strain and partial oxidation of manganese ions. Finally, reactions that involve vigorous gas evolution, such as the glycine nitrate process (GNP), often produce highly open nanostructured powders. However, it is worth to note that the detailed nanostructured of the powder depends on the combustion parameters.

In conclusion, the smallest and the most homogeneous $LiMn_2O_4$ nanoparticles with porous structure are the best materials to be used as cathodes, since the sum of these features would reduce the Jahn-Teller effect and the diffusion length for Li ions.

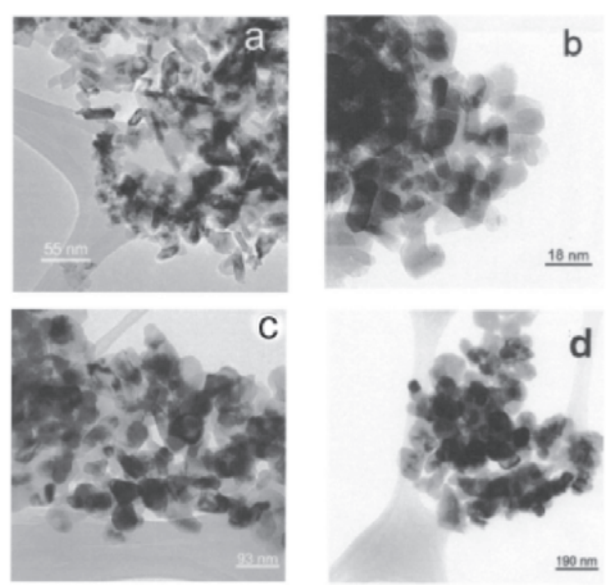

Figure 12. TEM photographs of $LiMn_2O_4$ spinels prepared by sol-gel annealed at different temperatures (a) 350 °C (b) 450 °C (c) 550 °C and (d) 650 °C. Reproduced with permission from © 2004, The Electrochemical Society, Inc.[27]

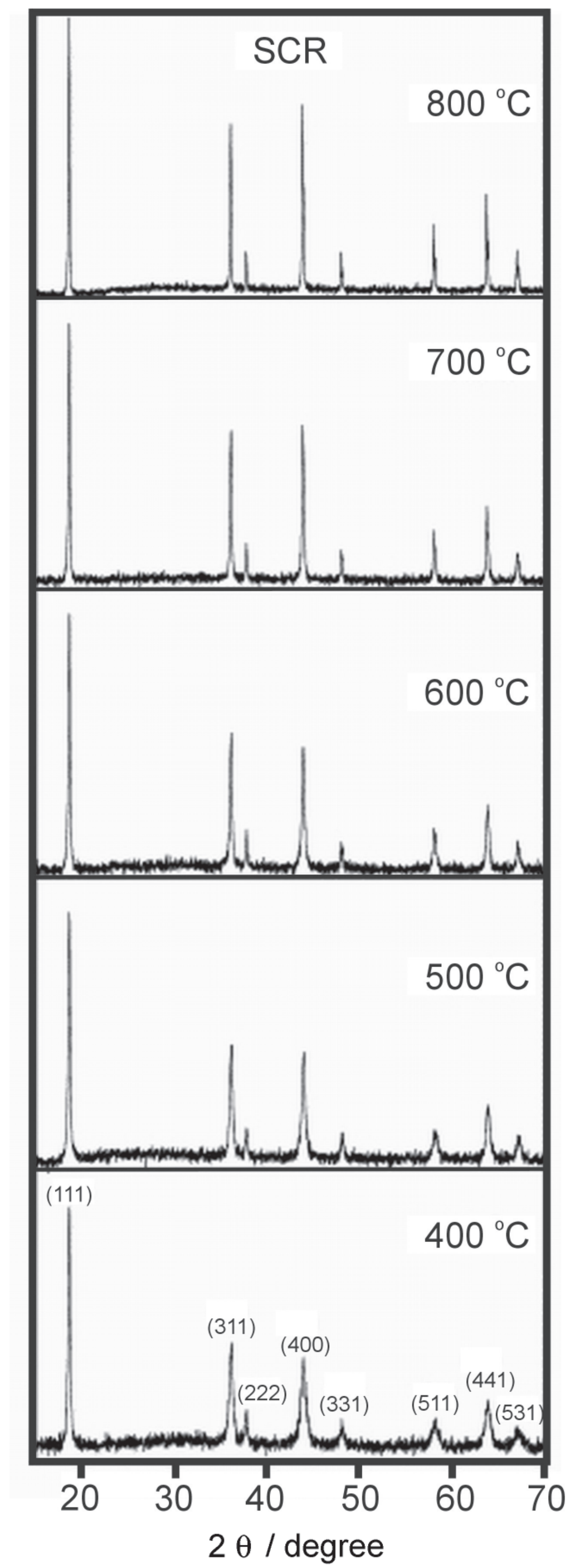

Figure 13. XRD spectra of spinel $LiMn_2O_4$ prepared by self-combustion reaction calcinated at different temperatures. Reprinted with permission from © 2004, Elsevier.[145]

There has been significant work over the last few years with the objective of optimizing the performance of the spinel $LiMn_2O_4$ by the substitution of different cations. Cations of Li, B, Mg, Al, Fe, Co, Ni and Zn have been investigated as possible dopants.[11,148-152]

Among these doped $LiMn_2O_4$ materials, $LiNi_{0.5}Mn_{1.5}O_2$ is one of the most studied.[153-156] The presence of Ni stabilizes the octahedral spinel sites and although the intercalation of lithium decreases the average valence of manganese to values below 4.5, the distortion of the tetrahedral phase is not observed. In addition, when the charge voltage increases above 4.3 V to 4.9 V, a new voltage plateau around 4.7 V appears, which suggest its use as cathode material for a 5V-lithium ion battery.[156, 157]

In general, $LiNi_{0.5}Mn_{1.5}O_2$ is produced by solid state reactions, where microparticles are obtained. In the last years, $LiNi_{0.5}Mn_{1.5}O_2$ nanoparticles were prepared by two different methods. Lee *et al.*[157] have prepared pure nanosized $LiNi_{0.5}Mn_{1.5}O_4$ powder by composite carbonate process, which is a combination of sol-gel and solid-state methods. Later, $LiNi_{0.5}Mn_{1.5}O_4$ spinel was synthesized by single step sucrose aided self-combustion method, where mesopores were observed among the particles.[158] In both cases, the samples are clusters (1-4 μm) composed of nano-sized small particles. When used as cathode in lithium ion batteries, discharge capacities around 140 mA h g^{-1} and excellent cyclability after several cycles were obtained in both cases. These nanosized materials have shown excellent electrochemical performance, even at high temperature, both in terms of cyclability and specific capacity.

When cobalt is added into spinel $LiMn_2O_4$ to afford $LiMn_{1.8}Co_{0.2}O_4$, this doping process also increases the stability of the spinel structure and consequently improves the cyclability. In addition, the conductivity of Co-doped $LiMn_2O_4$ is much higher than that of non-doped spinel manganese oxide.[159-161]

In general, this compound has been prepared by solid-state reactions and precipitation techniques. However, these synthetic methodologies have led to powders with large size and less controlled morphology.[151, 162]

$LiMn_{1.8}Co_{0.2}O_4$ nanoparticles (20-34 nm) were prepared via reverse micelle process,[163] followed by calcination. The smallest particles were obtained using water to oil ratio (W/O) around 1/5 and cathodes using these nanoparticles have shown excellent cyclability and good capacity (160 mA h g^{-1}). When larger W/O volume ratio was used and hence larger particles were obtained, the discharge capacity decreased markedly, besides the excellent cyclability.

In order to combine the superior electrochemical performance of layered structures with the advantages of a manganese-based chemistry, $LiMnO_2$ has appeared as a good substitute for spinel $LiMn_2O_4$ due to its higher theoretical capacity of 285 mA h g^{-1}.[164] In this compound, Li and Mn ions occupy octahedral sites arranged in an alternating zig-zag configuration of edge-sharing [LiO_6] and [MnO_6] octahedral. However, when $LiMnO_2$ is used as cathode in a Li-ion cell, it tends to transform toward the spinel structure only by a minor rearrangement of the cations and like spinel $LiMn_2O_4$ shows severe capacity fading with cycling.

As a way to overcome some of these difficulties encountered with crystalline $LiMnO_2$, amorphous or nanocrystalline structures have attracted increasing attention. In these structures it is believed that lattice stress caused by Jahn-Teller distortion can be accommodated more easily in disordered materials (amorphous) and in nanoarchitectures, exhibiting much higher Li intercalation capacity than their conventional crystalline counterparts.[165-170]

Wu *et al.*[171] have proposed a new method to prepare nanosized orthorhombic $LiMnO_2$ (35 nm) consisted by two-step liquid phase thermal process at low temperature. In the first step, the precursor Mn_3O_4 was prepared *via* a solvothermal route, where potassium permanganate powder was reduced with a primary alcohol, such as ethanol and methanol. Followed by hydrothermal process in lithium hydroxide aqueous solution at 160-180 °C, the precursor Mn_3O_4 was transformed to the nanocrystalline *o*-$LiMnO_2$. The initial charge-discharge curves are distinct from spinel phases, but the *o*-$LiMnO_2$ phase is transformed to spinel-like $LiMn_2O_4$ gradually. The cell using this material as cathode has shown initial reversible specific capacity of 225 mA h g^{-1} with moderate capacity fading (20%) after 30 cycles (Figure 14).

Later, nanosized orthorhombic $LiMnO_2$ with high purity and good crystallinity was synthesized by a simple

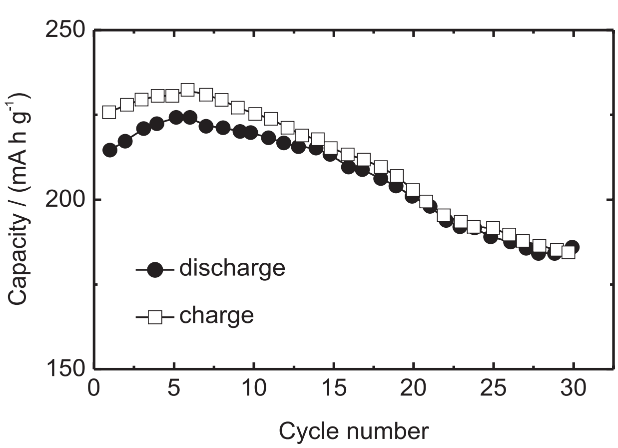

Figure 14. Charge and discharge capacities (mA h g^{-1}) of Li/*o*-$LiMnO_2$. Reprinted with permission from (c) 2004, Elsevier.[171]

process, involving controlled oxidation of $Mn(OH)_2$ followed by *in situ* exchange of lithium ions under mild conditions. The nanosized *o*-$LiMnO_2$ has exhibited excellent initial discharge capacity of 220 mA h g^{-1} with good cycling performance (89% retention after 30 cycles).[172]

So far, there are a limited number of methods to prepare nanocrystalline $LiMnO_2$, thereby this field research is still open to improvements.

It is interesting to state that the transformation from orthorhombic to spinel-like structure becomes easier when the degree of stacking faults increases. Thus, *o*-$LiMnO_2$ with a low number of stacking faults could display better cyclability than a high stacking faulted phase when cycled between 2.0 V and 4.3 V.

Therefore, nanomaterials with disordered lamellar structures are expected to play a role in inhibiting the rapid phase transformation observed in spinel $LiMn_2O_4$, because the irregular layer arrangement may provide a high-energy barrier against the phase conversion. So, besides nanoparticles and one-dimensional nanostructures such as nanotubes, nanowires and others, a variety of unilammelar 2-D crystallites have been synthesized by chemical delaminating a layered host into molecular single layers.[173-179] The resulting elementary layers, so-called "nanosheets" can act as inorganic building blocks to build up novel nanostructured systems. The restacking of these nanosheets via flocculation produces a disordered layered structure with irregular orientation (Figure 15). In 2003, colloidal MnO_2 nanosheets have been successfully obtained by delaminating an acid exchanged form of $KMnO_2$ with tetrabutylammonium (TBA) ions, followed by restacking via flocculation with lithium ions.[180] These nanosheets have shown high two-dimensionality associated with a thickness comparable to molecules, showing a number of interesting aspects with respect to highly two-dimensional anisotropy and ultra thin thickness in nanometer scale.

The resulting disordered sample underwent electrochemical Li^+ insertion/extraction with smooth cycling curves, showing specific capacity of 190 mA h g^{-1} in the first cycle, followed by 220 mA h g^{-1} in the next cycle and continuous decrease, as shown in Figure 16. After 20 cycles, only a very small plateau was showed at 4.0 V, but no apparent one at 3.0 V, which is characteristic of spinel phase, indicating the preservation of the initial phase. This smooth charge–discharge slope without well defined plateaus was apparently different of layered $LiMnO_2$, which generally undergoes phase transformation into spinel in the first cycles accompanied by evolution of a clear voltage profile feature of spinel structure with 3 V and 4 V. Probably, this capacity fading can be attributed

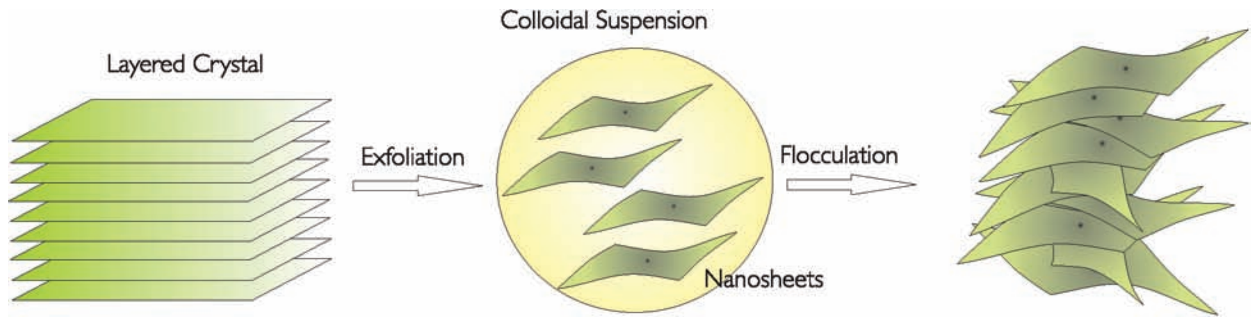

Figure 15. Procedure for fabrication nanosheets followed by flocculation.

to the formation of some inactive electrochemical phase or the dissolution of the material.

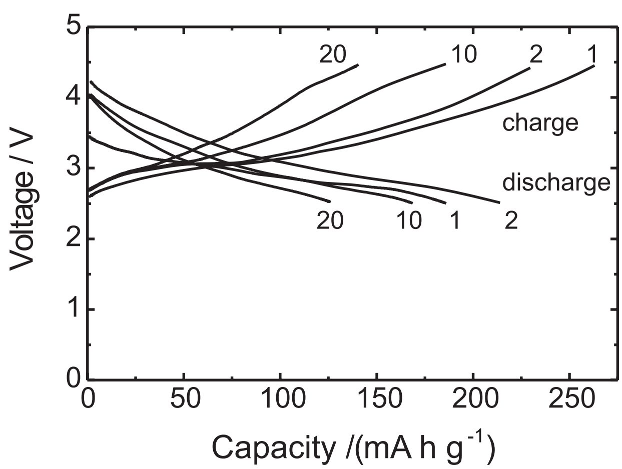

Figure 16. Discharge-charge curves of the restacked Li-Mn-oxide. Current density: 44 µA cm^{-2}. Reprint with permission from © 2004, American Chemical Society.[180]

6. Concluding Remarks

The use of nanomaterials for energy storage devices, such as batteries, is a rapidly growing field with tremendous potential. However, such research is only in its infancy and is likely to undergo dramatic evolutionary and revolutionary changes as insight into nanoarchitectures becomes clearer through scientific investigation in this research area.

In this review we present the motivations to use nanostructured transition metal oxides as cathodes in lithium ion batteries in place of the conventional microcrystalline ones. It is believed that such nanomaterials mitigate the problem of slow diffusion because the distance that lithium ion must diffuse in the solid state is limited to the radius of the nanoparticles. Moreover, nano-size particles have large surface area to volume ratio; therefore charge accommodations of these nanoscopic particles will take place largely at the surface, avoiding stress-induced structural changes (e.g. Jahn-Teller distortions in $Li_xMn_2O_4$).

To illustrate such advantages, several methodologies were presented as well as electrochemical data of the most used cathodes in nanoscale, such as $LiCoO_2$, $LiMn_2O_4$, $LiMnO_2$, LiV_2O_5 e $LiFePO_4$.

Acknowledgments

Fernanda F. C. Bazito thanks CNPq for the scholarship granted, Nº 151128-2004-9. We are also grateful to FAPESP (03/10015-3), CNPq and CNPq-IM2C2005 (420233/2005-9) for the financial support.

Roberto M. Torresi received his Ph.D. from the National University of Córdoba, Argentine (1986) and completed his postdoctoral training with Drs. M. Keddam and C. Gabrielli at the University Pierre et Marie Curie, Paris in 1990. His first faculty position was in the Department of Physical Chemistry at the Institute of Chemistry of São Carlos (USP) (1993). Dr. Torresi moved to the Institute of Chemistry at the University of São Paulo, in São Paulo city, in 2002, and he is Full Professor at the Department of Fundamental Chemistry. His research interests are electrochemistry of nanostructured electrodes and new electrolytes as ionic liquids.

Fernanda Ferraz Camilo Bazito received her Ph.D. from the University of São Paulo, Brazil (2002) and completed her postdoctoral training with Dr. D. Buttry at the University of Wyoming, Laramie in 2004. She has now a post-doctoral position at the Chemistry Institute of the University of São Paulo. Her research interests are new electroactive materials for nanotechnology and ionic liquids.

References

1. Nagaura, T.; Tozawa, K.; *Progress in Batteries & Solar Cells* **1990**, *9*, 209.
2. Sit, K.; Li, P. K. C.; Ip, C. W.; Wan, L.; Lai, P. Y.; Fan, J.; Magnuson, D.; *J. Power Sources* **2004**, *125*, 124.
3. Scrosati, B.; *Nature* **1995**, *373*, 557.
4. Thomas, J.; *Nat. Mat.* **2003**, *2*, 705.
5. Hammami, A.; Raymond, N.; Armand, M.; *Nature* **2003**, *424*, 635.
6. Besenhard, J. O.; Yang, J.; Winter, M.; *J. Power Sources* **1997**, *68*, 87.
7. Idota, Y.; Kubota, T.; Matsufuji, A.; Maekawa, Y.; Miyasaka, T.; *Science* **1997**, *276*, 1395.
8. Courtney, I. A.; Dahn, J. R.; *J. Electrochem. Soc.* **1997**, *144*, 2045.
9. Yamada, A.; Chung, S. C.; Hinokuma, K.; *J. Electrochem. Soc.* **2001**, *148*, A224.
10. Doeff, M. M.; Anapolsky, A.; Edman, L.; Richardson, T. J.; De Jonghe, L. C.; *J. Electrochem. Soc.* **2001**, *148*, A230.
11. Myung, S.-T.; Komaba, S.; Kumagai, N.; *J. Electrochem. Soc.* **2001**, *148*, A482.
12. Yamada, A.; Kudo, Y.; Liu, K.-Y.; *J. Electrochem. Soc.* **2001**, *148*, A747.
13. Mueller-Neuhaus, J. R.; Dunlap, R. A.; Dahn, J. R.; *J. Electrochem. Soc.* **2000**, *147*, 3598.
14. Ferracin, L. C.; Amaral, F. A.; Bocchi, N.; *Solid State Ionics* **2000**, *130*, 215.
15. Julien, C.; Gorenstein, A.; *J. Power Sources* **1995**, *15*, 373.
16. Lala, S. M.; Montoro, L. A.; Lemos, V.; Abbate, M.; Rosolen, J. M.; *Electrochim. Acta* **2005**, *51*, 7.
17. Huguenin, F.; Torresi, R. M.; *Quim. Nova* **2004**, *27*, 393.
18. Plichta, E. J.; Hendrickson, M.; Thompson, R.; Au, G.; Behl, W. K.; Smart, M. C.; Ratnakumar, B. V.; Surampudi, S.; *J. Power Sources* **2001**, *94*, 160.
19. Huang, H.; Wunder, S. L.; *J. Electrochem. Soc.* **2001**, *148*, A279.
20. Wang, X.; Yasukawa, E.; Kasuya, S.; *J. Electrochem. Soc.* **2001**, *148*, A1058.
21. Lee, K.-H.; Kim, K.-H.; Lim, H. S.; *J. Electrochem. Soc.* **2001**, *148*, A1148.
22. Smart, M. C.; Ratnakumar, B. V.; Surampudi, S.; *J. Electrochem. Soc.* **1999**, *146*, 486.
23. Sides, C. R.; Li, N.; Patrissi, C. J.; Scrosati, B.; Martin, C. R.; *MRS Bull.* **2002**, *27*, 604.
24. Scrosati, B.; *Electrochim. Acta* **2000**, *45*, 2461.
25. Li, N.; Martin, C. R.; Scrosati, B.; *J. Power Sources* **2001**, *97-98*, 240.
26. Odani, A.; Nimberger, A.; Markovsky, B.; Sominski, E.; Levi, E.; Kumar, V. G.; Motiei, M.; Gedanken, A.; Dan, P.; Aurbach, D.; *J. Power Sources* **2003**, *119-121*, 517.
27. Curtis, C. J.; Wang, J.; Schulz, D. L.; *J. Electrochem. Soc.* **2004**, *151*, A590.
28. Jamnik, J.; Maier, J.; *Phys. Chem. Chem. Phys.* **2003**, *5*, 5215.
29. Bueno, P. R.; Leite, E. R.; *J. Phys. Chem. B* **2003**, *107*, 8868.
30. Granasy, L.; Igloi, F.; *J. Chem. Phys.* **1997**, *107*, 3634.
31. Dong, W.; Rolison, D. R.; Dunn, B.; *Electrochem. Solid-State Lett.* **2000**, *3*, 457.
32. Kavan, L.; Rathousky, J.; Gratzel, M.; Shklover, V.; Zukal, A.; *J. Phys. Chem. B* **2000**, *104*, 12012.
33. Vivier, V.; Farcy, J.; Pereira-Ramos, J. P.; *Electrochim. Acta* **1998**, *44*, 831.
34. Mizushima, K.; Jones, P. C.; Wiseman, P. J.; Goodenough, J. B.; *MRS Bull.* **1980**, *15*, 783.
35. Liu, H.; Wu, Y. P.; Rahm, E.; Holze, R.; Wu, H. Q.; *J. Solid State Electrochem.* **2004**, *8*, 450.
36. Whittingham, M. S.; *Chem. Rev.* **2004**, *104*, 4271.
37. Makhonina, E. V.; Pervov, V. S.; Dubasova, V. S.; *Russ. Chem Rev.* **2004**, *73*, 991.
38. Fey, G. T.-K.; Huang, D.-L.; *Electrochim. Acta* **1999**, *45*, 295.
39. Thackeray, M. M.; *J. Am. Ceram. Soc.* **1999**, *82*, 3347.
40. Padhi, A. K.; Nanjundaswamy, K. S.; Goodenough, J. B.; *J. Electrochem. Soc.* **1997**, *144*, 1188.
41. Thackeray, M. M.; *Nat. Mat.* **2002**, *1*, 81.
42. Ouyang, C.; Shi, S.; Wang, Z.; Huang, X.; Chen, L.; *Phys. Rev. B* **2004**, *69*, 104303.
43. MacNeil, D. D.; Lu, Z.; Chen, Z.; Dahn, J. R.; *J. Power Sources* **2002**, *108*, 8.
44. Takahashi, M.; Tobishima, S.-I.; Takei, K.; Sakurai, Y.; *Solid State Ionics* **2002**, *148*, 283.
45. Hu, Y.; Doeff, M. M.; Kostecki, R.; Finones, R.; *J. Electrochem. Soc.* **2004**, *151*, A1279.
46. Prosini, P. P.; Zane, D.; Pasquali, M.; *Electrochim. Acta* **2001**, *46*, 3517.
47. Okada, S.; Sawa, S.; Egashira, M.; Yamaki, J. i.; Tabuchi, M.; Kageyama, H.; Konishi, T.; Yoshino, A.; *J. Power Sources* **2001**, *97-98*, 430.
48. Takahashi, M.; Tobishima, S.; Takei, K.; Sakurai, Y.; *J. Power Sources* **2001**, *97-98*, 508.
49. Prosini, P. P.; Carewska, M.; Scaccia, S.; Wisniewski, P.; Passerini, S.; Pasquali, M.; *J. Electrochem. Soc.* **2002**, *149*, A886.
50. Singhal, A.; Skandan, G.; Amatucci, G.; Badway, F.; Ye, N.; Manthiram, A.; Ye, H.; Xu, J. J.; *J. Power Sources* **2004**, *129*, 38.
51. Chung, H.-T.; Jang, S.-K.; Ryu, H. W.; Shim, K.-B.; *Solid State Commun.* **2004**, *131*, 549.
52. Myung, S.-T.; Komaba, S.; Hirosaki, N.; Yashiro, H.; Kumagai, N.; *Electrochim. Acta* **2004**, *49*, 4213.
53. Hsu, K.-F.; Tsay, S.-Y.; Hwang, B.-J.; *J. Mater. Chem.* **2004**, *14*, 2690.

54. Chen, Z.; Dahn, J. R.; *J. Electrochem. Soc.* **2002**, *149*, A1184.
55. Murphy, D. W.; Christian, P. A.; DiSalvo, F. J.; Carides, J. N.; *J. Electrochem. Soc.* **1979**, *126*, 497.
56. Tsang, C.; Manthiram, A.; *J. Electrochem. Soc.* **1997**, *144*, 520.
57. Bergstrom, O.; Gustafsson, T.; Thomas, J. O.; *Acta Crystallogr., Sect. C: Cryst. Struct. Commun.* **1998**, *C54*, 1204.
58. Liu, G. Q.; Zeng, C. L.; Yang, K.; *Electrochim. Acta* **2002**, *47*, 3239.
59. Passerini, S.; Ressler, J. J.; Le, D. B.; Owens, B. B.; Smyrl, W. H.; *Electrochim. Acta* **1999**, *44*, 2209.
60. Huguenin, F.; Torresi, R. M.; Buttry, D. A.; *J. Electrochem. Soc.* **2002**, *149*, A546.
61. Coustier, F.; Passerini, S.; Smyrl, W. H.; *J. Electrochem. Soc.* **1998**, *145*, L73.
62. Salloux, K.; Chaput, F.; Wong, H. P.; Dunn, B.; Breiter, M. W.; *J. Electrochem. Soc.* **1995**, *142*, L191.
63. Coustier, F.; Hill, J.; Owens, B. B.; Passerini, S.; Smyrl, W. H.; *J. Electrochem. Soc.* **1999**, *146*, 1355.
64. Park, H. K.; Smyrl, W. H.; Ward, M. D.; *J. Electrochem. Soc.* **1995**, *142*, 1068.
65. Le, D. B.; Passerini, S.; Tipton, A. L.; Owens, B. B.; Smyrl, W. H.; *J. Electrochem. Soc.* **1995**, *142*, L102.
66. Huguenin, F.; Torresi, R. M.; *J. Braz. Chem. Soc.* **2003**, *14*, 536.
67. Huguenin, F.; Torresi, R. M.; Buttry, D. A.; Pereira da Silva, J. E.; Cordoba de Torresi, S. I.; *Electrochim. Acta* **2001**, *46*, 3555.
68. Huguenin, F.; Giz, M. J.; Ticianelli, E. A.; Torresi, R. M.; *J. Power Sources* **2001**, *103*, 113.
69. Huguenin, F.; Do Prado Gambardella, M. T.; Torresi, R. M.; De Torresi, S. I. C.; Buttry, D. A.; *J. Electrochem. Soc.* **2000**, *147*, 2437.
70. Wong, H. P.; Dave, B. C.; Leroux, F.; Harreld, J.; Dunn, B.; Nazar, L. F.; *J. Mater. Chem.* **1998**, *8*, 1019.
71. Goward, G. R.; Leroux, F.; Nazar, L. F.; *Electrochim. Acta* **1998**, *43*, 1307.
72. Liu, Y. J.; Schindler, J. L.; DeGroot, D. C.; Kannewurf, C. R.; Hirpo, W.; Kanatzidis, M. G.; *Chem. Mater.* **1996**, *8*, 525.
73. Leroux, F.; Koene, B. E.; Nazar, L. F.; *J. Electrochem. Soc.* **1996**, *143*, L181.
74. Wu, C. G.; DeGroot, D. C.; Marcy, H. O.; Schindler, J. L.; Kannewurf, C. R.; Liu, Y. J.; Hirpo, W.; Kanatzidis, M. G.; *Chem. Mater.* **1996**, *8*, 1992.
75. Demets, G. J. F.; Anaissi, F. J.; Toma, H. E.; *Electrochim. Acta* **2000**, *46*, 547.
76. Kuwabata, S.; Masui, S.; Tomiyori, H.; Yoneyama, H.; *Electrochim. Acta* **2000**, *46*, 91.
77. Somani, P. R.; Marimuthu, R.; Mandale, A. B.; *Polymer* **2001**, *42*, 2991.
78. Malta, M.; Louarn, G.; Errien, N.; Torresi, R. M.; *Electrochem. Commun.* **2003**, *5*, 1011.
79. Wang, Y. W.; Xu, H. Y.; Wang, H.; Zhang, Y. C.; Song, Z. Q.; Yan, H.; Wan, C. R.; *Solid State Ionics* **2004**, *167*, 419.
80. Xu, H. Y.; Wang, H.; Song, Z. Q.; Wang, Y. W.; Zhang, Y. C.; Yan, H.; *Chem. Lett.* **2003**, *32*, 444.
81. Patrissi, C. J.; Martin, C. R.; *J. Electrochem. Soc.* **2001**, *148*, A1247.
82. Spahr, M. E.; Bitterli, P.; Nesper, R.; Muller, M.; Krumeich, F.; Nissen, H. U.; *Angew. Chem., Int. Ed.* **1998**, *37*, 1263.
83. Nordlinder, S.; Edstrom, K.; Gustafsson, T.; *Electrochem. Solid-State Lett.* **2001**, *4*, A129.
84. Patrissi, C. J.; Martin, C. R.; *J. Electrochem. Soc.* **1999**, *146*, 3176.
85. Niederberger, M.; Muhr, H.-J.; Krumeich, F.; Bieri, F.; Guenther, D.; Nesper, R.; *Chem. Mater.* **2000**, *12*, 1995.
86. Sakamoto, J. S.; Dunn, B.; *J. Electrochem. Soc.* **2002**, *149*, A26.
87. Dong, W.; Sakamoto, J. S.; Dunn, B.; *Sci. Technol. Adv. Mater.* **2003**, *4*, 3.
88. Besenhard, J. O.; Schollhorn, R.; *J. Power Sources* **1976**, *1*, 267.
89. Schollhorn, R.; Klein-Reesink, F.; Reimold, R.; *J. Chem. Soc., Chem. Commun.* **1979**, *1979*, 398.
90. Yu, A.; Kumagai, N.; Liu, Z.; Lee, J. Y.; *J. Power Sources* **1998**, *74*, 117.
91. Kawakita, J.; Kato, T.; Katayama, Y.; Miura, T.; Kishi, T.; *J. Power Sources* **1999**, *81-82*, 448.
92. West, K.; Zachau-Christiansen, B.; Skaarup, S.; Saidi, Y.; Barker, J.; Olsen, I. I.; Pynenburg, R.; Koksbang, R.; *J. Electrochem. Soc.* **1996**, *143*, 820.
93. Pistoia, G.; Pasquali, M.; Wang, G.; Li, L.; *J. Electrochem. Soc.* **1990**, *137*, 2365.
94. Pistoia, G.; Pasquali, M.; Tocci, M.; Manev, V.; Moshtev, R.; *J. Power Sources* **1985**, *15*, 13.
95. Xu, H. Y.; Wang, H.; Song, Z. Q.; Wang, Y. W.; Yan, H.; Yoshimura, M.; *Electrochim. Acta* **2004**, *49*, 349.
96. Manev, V.; Momchilov, A.; Nassalevska, A.; Pistoia, G.; Pasquali, M.; *J. Power Sources* **1995**, *54*, 501.
97. Kumagai, N.; Yu, A.; *J. Electrochem. Soc.* **1997**, *144*, 830.
98. Chirayil, T. A.; Zavalij, P. Y.; Whittingham, M. S.; *J. Electrochem. Soc.* **1996**, *143*, L193.
99. Swider-Lyons, K. E.; Love, C. T.; Rolison, D. R.; *Solid State Ionics* **2002**, *152-153*, 99.
100. Kannan, A. M.; Manthiram, A.; *Solid State Ionics* **2003**, *159*, 265.
101. Christian, P. A.; DiSalvo, F. J.; Murphy, D. W.*; BE Pat. 879278*, **1980**.
102. Chen, W.; Peng, J.; Mai, L.; Yu, H.; Qi, Y.; *Chem. Lett.* **2004**, *33*, 1366.
103. Striebel, K. A.; Deng, C. Z.; Wen, S. J.; Cairns, E. J.; *J. Electrochem. Soc.* **1996**, *143*, 1821.
104. Zhecheva, E.; Stoyanova, R.; Gorova, M.; Alcantara, R.; Morales, J.; Tirado, J. L.; *Chem. Mater.* **1996**, *8*, 1429.
105. Kang, S. G.; Kang, S. Y.; Ryu, K. S.; Chang, S. H.; *Solid State Ionics* **1999**, *120*, 155.

106. Sun, Y.-K.; *J. Power Sources* **1999**, *83*, 223.
107. Peng, Z. S.; Wan, C. R.; Jiang, C. Y.; *J. Power Sources* **1998**, *72*, 215.
108. Fey, G. T. K.; Chen, K. S.; Hwang, B. J.; Lin, Y. L.; *J. Power Sources* **1997**, *68*, 519.
109. Sun, Y.-K.; Oh, I.-H.; Hong, S.-A.; *J. Mater. Sci.* **1996**, *31*, 3617.
110. Lu, C.-H.; Yeh, P.-Y.; *J. Mater. Chem.* **2000**, *10*, 599.
111. Myung, S. T.; Kumagai, N.; Komaba, S.; Chung, H. T.; *J. Appl. Electrochem.* **2000**, *30*, 1081.
112. Chen, C.; Kelder, E. M.; van der Put, P. J. J. M.; Schoonman, J.; *J. Mater. Chem.* **1996**, *6*, 765.
113. Chen, C. H.; Kelder, E. M.; Schoonman, J.; *J. Mater. Sci.* **1996**, *31*, 5437.
114. Chen, C. H.; Buysman, A. A. J.; Kelder, E. M.; Schoonman, J.; *Solid State Ionics* **1995**, *80*, 1.
115. Wu, Q.; Li, W.; Cheng, Y.; Jiang, Z.; *Mater. Chem. Phys.* **2005**, *91*, 463.
116. Chen, H.; Qiu, X.; Zhu, W.; Hagenmuller, P.; *Electrochem. Commun.* **2002**, *4*, 488.
117. Leising, R. A.; Palazzo, M. J.; Takeuchi, E. S.; Takeuchi, K. J.; *J. Power Sources* **2001**, *97-98*, 681.
118. Maleki, H.; Hallaj, S. A.; Selman, J. R.; Dinwiddie, R. B.; Wang, H.; *J. Electrochem. Soc.* **1999**, *146*, 947.
119. Liu, L.; Wang, Z.; Li, H.; Chen, L.; Huang, X.; *Solid State Ionics* **2002**, *152-153*, 341.
120. Mladenov, M.; Stoyanova, R.; Zhecheva, E.; Vassilev, S.; *Electrochem. Commun.* **2001**, *3*, 410.
121. Park, S.-C.; Kim, Y.-M.; Kang, Y.-M.; Kim, K.-T.; Lee, P. S.; Lee, J.-Y.; *J. Power Sources* **2001**, *103*, 86.
122. Cho, J.; Kim, G.; *Electrochem. Solid-State Lett.* **1999**, *2*, 253.
123. Cho, J.; Kim, H.; Park, B.; *J. Electrochem. Soc.* **2004**, *151*, A1707.
124. Cho, J.; *Electrochem. Commun.* **2003**, *5*, 146.
125. Cho, J.; *Electrochim. Acta* **2003**, *48*, 2807.
126. Cho, J.; Kim, Y.-W.; Kim, B.; Lee, J.-G.; Park, B.; *Angew. Chem., Int. Ed.* **2003**, *42*, 1618.
127. Zhao, H.; Gao, L.; Qiu, W.; Zhang, X.; *J. Power Sources* **2004**, *132*, 195.
128. Wakihara, M.; *Mater. Sci. Eng., R Rep.* **2001**, *R33*, 109.
129. Ohzuku, T.; Kitagawa, M.; Hirai, T.; *J. Electrochem. Soc.* **1990**, *137*, 40.
130. Koksbang, R.; Barker, J.; Saiedi, M. Y.; West, K.; Zachau-Christiansen, B.; Skaarup, S.; *Solid State Ionics* **1996**, *83*, 151.
131. Gummow, R. J.; De Kock, A.; Thackeray, M. M.; *Solid State Ionics* **1994**, *69*, 59.
132. Jiang, Z.; Abraham, K. M.; *J. Electrochem. Soc.* **1996**, *143*, 1591.
133. Tarascon, J. M.; McKinnon, W. R.; Coowar, F.; Bowmer, T. N.; Amatucci, G.; Guyomard, D.; *J. Electrochem. Soc.* **1994**, *141*, 1421.
134. Thackeray, M. M.; Johnson, P. J.; De Picciotto, L. A.; Bruce, P. G.; Goodenough, J. B.; *MRS Bull.* **1984**, *19*, 179.
135. Tarascon, J. M.; Wang, E.; Shokoohi, F. K.; McKinnon, W. R.; Colson, S.; *J. Electrochem. Soc.* **1991**, *138*, 2859.
136. Manev, V.; Momchilov, A.; Nassalevska, A.; Sato, A.; *J. Power Sources* **1995**, *54*, 323.
137. Guan, J.; Liu, M.; *Solid State Ionics* **1998**, *110*, 21.
138. Nieto, S.; Majumder, S. B.; Katiyar, R. S.; *J. Power Sources* **2004**, *136*, 88.
139. Kumar, V. G.; Gnanaraj, J. S.; Ben-David, S.; Pickup, D. M.; Van-Eck, E. R. H.; Gedanken, A.; Aurbach, D.; *Chem. Mater.* **2003**, *15*, 4211.
140. Choy, J. H.; Kim, D. H.; Kwon, C. W.; Hwang, S. J.; Kim, Y. I.; *J. Power Sources* **1999**, *77*, 1.
141. Taniguchi, I.; Lim, C. K.; Song, D.; Wakihara, M.; *Solid State Ionics* **2002**, *146*, 239.
142. Hwang, B. J.; Santhanam, R.; Liu, D. G.; *J. Power Sources* **2001**, *97-98*, 443.
143. Lucas, P.; Angell, C. A.; *J. Electrochem. Soc.* **2000**, *147*, 4459.
144. Choi, H. J.; Lee, K. M.; Kim, G. H.; Lee, J. G.; *J. Am. Ceram. Soc.* **2001**, *84*, 242.
145. Gadjov, H.; Gorova, M.; Kotzeva, V.; Avdeev, G.; Uzunova, S.; Kovacheva, D.; *J. Power Sources* **2004**, *134*, 110.
146. Zhang, Y.; Shin, H.-C.; Dong, J.; Liu, M.; *Solid State Ionics* **2004**, *171*, 25.
147. Kang, S.-H.; Goodenough, J. B.; Rabenberg, L. K.; *Electrochem. Solid-State Lett.* **2001**, *4*, A49.
148. Kaneko, M.; Matsuno, S.; Miki, T.; Nakayama, M.; Ikuta, H.; Uchimoto, Y.; Wakihara, M.; Kawamura, K.; *J. Phys. Chem. B* **2003**, *107*, 1727.
149. Lee, J. H.; Hong, J. K.; Jang, D. H.; Sun, Y. K.; Oh, S. M.; *J. Power Sources* **2000**, *89*, 7.
150. Amine, K.; Tukamoto, H.; Yasuda, H.; Fujita, Y.; *J. Power Sources* **1997**, *68*, 604.
151. Banov, B.; Todorov, Y.; Trifonova, A.; Momchilov, A.; Manev, V.; *J. Power Sources* **1997**, *68*, 578.
152. Myung, S.-T.; Komaba, S.; Kumagai, N.; Yashiro, H.; Chung, H.-T.; Cho, T.-H.; *Electrochim. Acta* **2002**, *47*, 2543.
153. Alcantara, R.; Jaraba, M.; Lavela, P.; Tirado, J. L.; *Electrochim. Acta* **2002**, *47*, 1829.
154. Sun, Y. K.; Hong, K. J.; Prakash, J.; Amine, K.; *Electrochem. Commun.* **2002**, *4*, 344.
155. Mohamedi, M.; Makino, M.; Dokko, K.; Itoh, T.; Uchida, I.; *Electrochim. Acta* **2002**, *48*, 79.
156. Zhong, Q.; Banakdarpour, A.; Zhang, M.; Gao, Y.; Dahn, J. R.; *J. Electrochem. Soc.* **1997**, *144*, 205.
157. Lee, Y. S.; Sun, Y. K.; Ota, S.; Miyashita, T.; Yoshio, M.; *Electrochem. Commun.* **2002**, *4*, 989.
158. Lazarraga, M. G.; Pascual, L.; Gadjov, H.; Kovacheva, D.; Petrov, K.; Amarilla, J. M.; Rojas, R. M.; Martin-Luengo, M. A.; Rojo, J. M.; *J. Mater. Chem.* **2004**, *14*, 1640.

159. Arora, P.; Popov, B. N.; White, R. E.; *J. Electrochem. Soc.* **1998**, *145*, 807.
160. Chang, S. H.; Ryu, K. S.; Kim, K. M.; Kim, M. S.; Kim, I. K.; Kang, S. G.; *J. Power Sources* **1999**, *84*, 134.
161. Amarilla, J. M.; De Vidales, J. L. M.; Rojas, R. M.; *Solid State Ionics* **2000**, *127*, 73.
162. Franger, S.; Bach, S.; Pereira-Ramos, J. P.; Baffier, N.; *J. Electrochem. Soc.* **2000**, *147*, 3226.
163. Lu, C.-H.; Wang, H.-C.; *J. Eur. Ceram. Soc.* **2003**, *23*, 865.
164. Bruce, P. G.; Armstrong, A. R.; Gitzendanner, R. L.; *J. Mater. Chem.* **1999**, *9*, 193.
165. Leroux, F.; Nazar, L. F.; *Solid State Ionics* **1997**, *100*, 103.
166. Kim, S. H.; Kim, S. J.; Oh, S. M.; *Chem. Mater.* **1999**, *11*, 557.
167. Xu, J. J.; Kinser, A. J.; Owens, B. B.; Smyrl, W. H.; *Electrochem. Solid-State Lett.* **1998**, *1*, 1.
168. Passerini, S.; Coustier, F.; Giorgetti, M.; Smyrl, W. H.; *Electrochem. Solid-State Lett.* **1999**, *2*, 483.
169. Palos, A. I.; Anne, M.; Strobel, P.; *Solid State Ionics* **2001**, *138*, 203.
170. Xu, J. J.; Jain, G.; Yang, J.; *Electrochem. Solid-State Lett.* **2002**, *5*, A152.
171. Wu, M.; Zhang, Q.; Lu, H.; Chen, A.; *Solid State Ionics* **2004**, *169*, 47.
172. Li, X.-D.; Yang, W.-S.; Zhang, S.-C.; Evans, D. G.; Duan, X.; *Solid State Ionics* **2005**, *176*, 803.
173. Sasaki, T.; Watanabe, M.; *J. Am. Chem. Soc.* **1998**, *120*, 4682.
174. Sasaki, T.; Watanabe, M.; Hashizume, H.; Yamada, H.; Nakazawa, H.; *J. Am. Chem. Soc.* **1996**, *118*, 8329.
175. Kaschak, D. M.; Johnson, S. A.; Hooks, D. E.; Kim, H.-N.; Ward, M. D.; Mallouk, T. E.; *J. Am. Chem. Soc.* **1998**, *120*, 10887.
176. Zhang, Z.; Lerner, M. M.; *Chem. Mater.* **1996**, *8*, 257.
177. Wang, Z.; Pinnavaia, T. J.; *Chem. Mater.* **1998**, *10*, 1820.
178. Han, Y.-S.; Park, I.; Choy, J.-H.; *J. Mater. Chem.* **2001**, *11*, 1277.
179. Liu, Z.-h.; Ooi, K.; Kanoh, H.; Tang, W.-P.; Tomida, T.; *Langmuir* **2000**, *16*, 4154.
180. Wang, L.; Takada, K.; Kajiyama, A.; Onoda, M.; Michiue, Y.; Zhang, L.; Watanabe, M.; Sasaki, T.; *Chem. Mater.* **2003**, *15*, 4508.

Received: November 1, 2005
Published on the web: May 16, 2006

FAPESP helped in meeting the publication costs of this article.